Evaluation of Point Spread Function and Functional Sensitivity of 3D-GRASE and 2D Spin-Echo EPI for Sub-Millimeter-Resolution fMRI at 7 T

Valentin G. Kemper[1], Federico De Martino[1], An T. Vu[2], Benedikt A. Poser[1], David A. Feinberg[3,4], Essa Yacoub[2], and Rainer Goebel[1]

[1]*Department of Cognitive Neuroscience, Maastricht University, Maastricht, Limburg, Netherlands,* [2]*Radiology, Center for Magnetic Resonance Research, University of Minnesota, Minneapolis, Minnesota, United States,* [3]*Helen Wills Institute of Neuroscience, University of California, Berkeley, United States,* [4]*Advanced MRI Technologies, California, United States*

Target Audience. MR physicists and researchers interested in ultra-high field and high-resolution fMRI

Purpose. This study sets out to compare Spin-Echo Echo Planar Imaging (SE-EPI) and Inner Volume Selective 3D Gradient-and-Spin-Echo (3D-GRASE [1,2]) sequences with regard to sensitivity and resolution in the context of high spatial resolution fMRI at ultra-high field strength.

Methods & Results. All experiments were performed on a 7 Tesla Siemens Magnetom scanner with a body gradient coil (70 mT/m, 200 mT/m/s) and a dedicated half-volume (16 channel (Rx; quadrature Tx) radio frequency head coil array. A visual stimulation (8 Hz flickering checkerboards) block design with 14 blocks of 10 s stimulation and 12 s rest was chosen. Three healthy volunteers were scanned in agreement with local ethical approval. Five different acquisitions were performed (two runs each): two 3D-GRASE acquisitions (TE= 36ms, acquisition time 240 ms) with orthogonal slice orientation (rotated about the readout direction), and three SE-EPI (TE=36 ms, GRAPPA R=2; TE=50 ms, R=2; and TE=50 ms, R=3). In the vendor–provided SE-EPI sequence the RF pulse lengths and the polarity of the slice-select gradient were modified to lower SAR and for low-SAR fat suppression. All functional data were acquired at a nominal isotropic resolution of 0.8 mm and a base matrix size of 120. The phase FoV was 25%/100% in the 3D-GRASE/SE-EPI case. Partial Fourier acquisition of 5/8 (3D-GRASE, partition direction, center-out acquisition) and 6/8 (SE-EPI, phase encoding direction) was used. Other imaging parameters for 3D-GRASE/SE-EPI: slices 10/16, echo spacing 1.01/1.02-1.03 ms, phase encoding lines, 30/30-45.

The data were analyzed using BrainVoyager QX 2.8, MATLAB, and FSL routines. We simulated the signal evolution along the echo train based on literature T2 and T2* of cortical gray matter in order to model the T2/T2* blurring due to signal decay. This T2/T2* decay was compared to imaging scans in which all phase encoding gradients were switched off. Fig. 1 shows the estimated FWHM of a Lorentzian function (nonlinear least-squares regression, 2 free parameters). In addition, we estimated blurring in residual noise images (after removal of the BOLD response) in the readout-, phase-, and slice-direction, using the FSL 'smoothest' routine (Fig. 1 bottom). This procedure estimates the width of a spatial Gaussian filter kernel [3,4].

A GLM analysis was conducted after the data were high-pass filtered and motion-corrected (SE-EPI additionally slice-time corrected, Fig. 2). Number of activated voxels in mutual volume (one-tailed t-test, p<0.05 (Bonferroni-corrected): 3D-GRASE 1: 1488, 3D-GRASE 2: 1402, SE-EPI 1: 201, SE-EPI 2: 128, SE-EPI 3: 57. After alignment to high-resolution T1-weighted anatomical images we conducted cortical layer-profiles of the activity in the jointly covered parts of visual cortex (not shown).

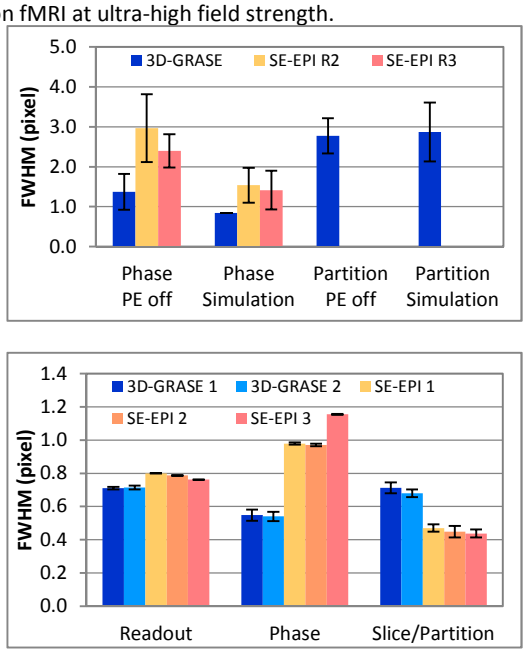

Fig. 1: Estimates of point spread function. Top: FWHM of Lorentzian function fitted to data, in which phase encoding gradients were switched off (PE off), and simulated data. Bottom: FWHM of a Gaussian kernel from smoothest in all imaging directions.

Discussion. Despite the relatively long echo train of the 3D-GRASE the point-spread in the partition direction is comparable to the point-spread in the 2D SE-EPI in the phase-encoding direction. The point-spread in the in-plane phase encoding direction in 3D-GRASE is particularly small, whereas larger required phase FoVs result in larger phase encoding PSFs in 2D SE-EPI (multi-slice acquisition is incompatible with 2D inner volume selection, requiring large FoV acquisitions (to avoid folding-in); partial Fourier is needed to reduce echo time which is achieved in 3D GRASE with centric ordering of the phase encoding along the partition direction). Blurring in readout direction is virtually constant across the different sequences (differences likely attributable to slightly different ramp sampling). The results of the two orthogonal 3D-GRASE acquisitions do not reflect any residual underlying anatomical information (Fig. 1 bottom).

Strong visual activation, which is confined to gray matter voxels, can be seen in all acquisitions. t-values are higher in 3D-GRASE because of the high temporal signal to noise ratio, however, volumetric coverage is more limited. SE-EPI data is more distorted, especially the R=2 data (Fig. 2c).

Simulations and non-phase encoded scans are in good agreement for the partition direction of 3D-GRASE, but differ for the phase-encoding direction. One possible explanation is imperfections induced by off-resonance, which the gradient echoes in the EPI-readout are more prone to, and additionally partial Fourier acquisition in 2D SE-EPI.

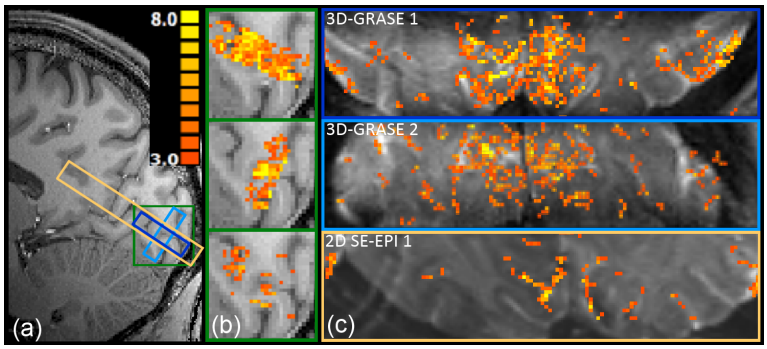

Fig. 2: a) anatomical reference from T1-weighted MP-RAGE with superimposed slab positions of functional scans. b) sagittal view of functional activity maps from 3D-GRASE (top: traversal slice orientation, center: coronal slice orientation) and 2D SE-EPI (bottom: TE=36 ms, R=2) overlaid on same anatomical slice. c) single slice functional activity maps in-plane superimposed on time-series average of functional scans (in-plane) in a representative subject (same order as b). All maps thresholded to same window of t-values, only three out of five acquisition types shown.

References. [1] Feinberg DA Radiology 1985;156:743. [2]Feinberg DA Proc. ISMRM 16; 2008. [3]Flitney DE, Jenkinson M, FMRIB Technical Report TR00DF1; 2000. [4]Nichols TE, FMRIB Technical Report TR08TN1; 2008.